Supplemental Figure 1

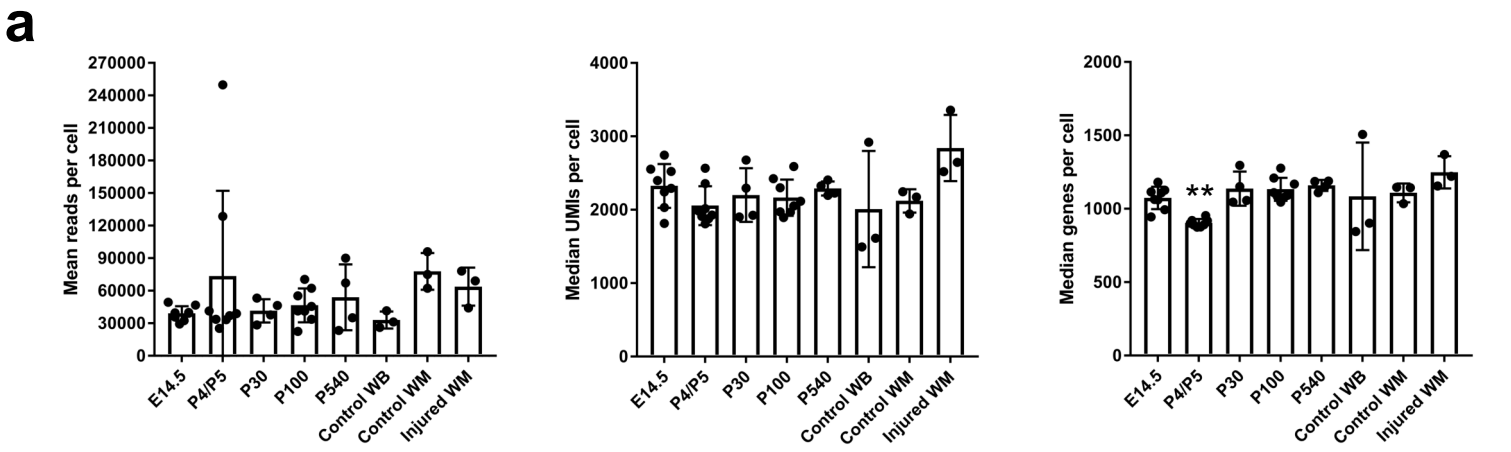

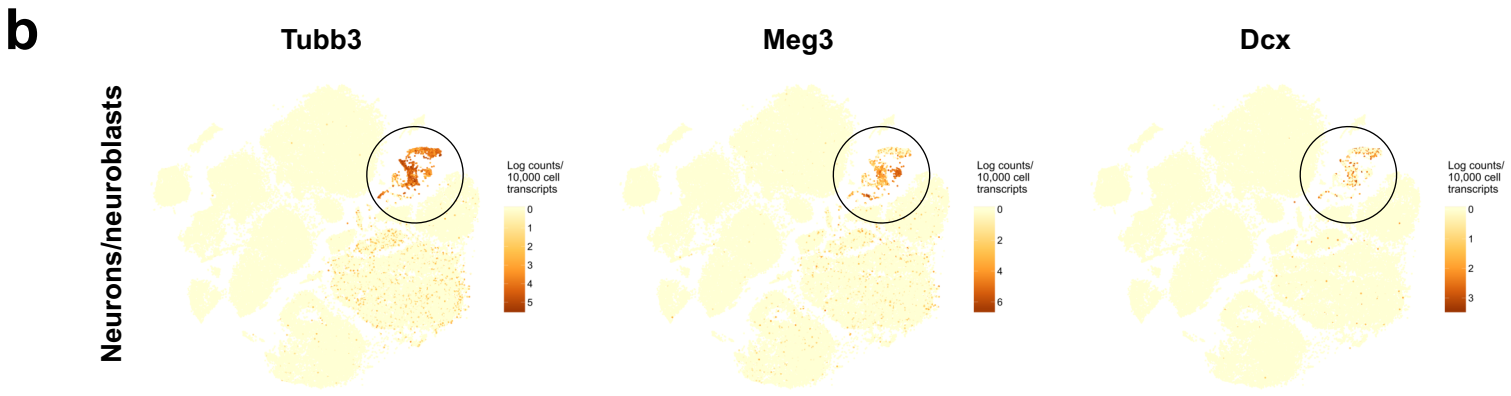

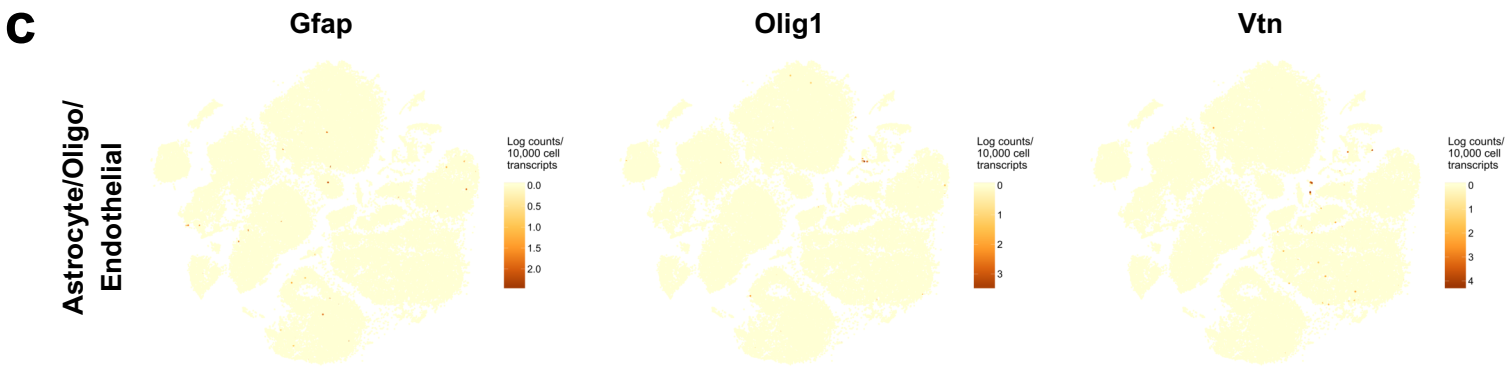

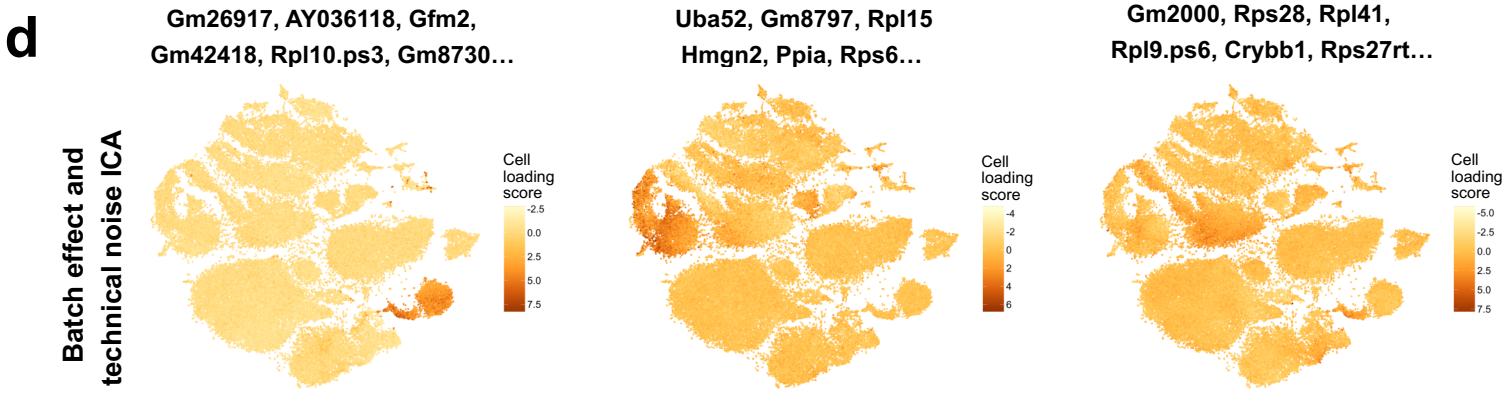

Figure S1. Percoll has no major effect on the subpopulations of microglia isolated from the brain, related to STAR methods.

(a) tSNE plot of microglia from P5 female mice (N=3 per age) that were purified with and without Percoll shows nine microglia clusters.

(b) tSNE plots of cells from each condition.

(c) tSNE plot of all cells colored for expression (log-transformed UMI counts per 10,000 transcripts) of *Spp1*, which was enriched in Cluster 8, which was less represented in the Percoll-purified samples.

(d) Plot of the normalized percent of cells from each sample assigned to each cluster. Green dotted line denotes the expected 50% of cells per cluster if equally represented in both conditions. ****P<0.0001, Two-way ANOVA, Tukey's post-hoc analysis.

Supplemental Figure 2

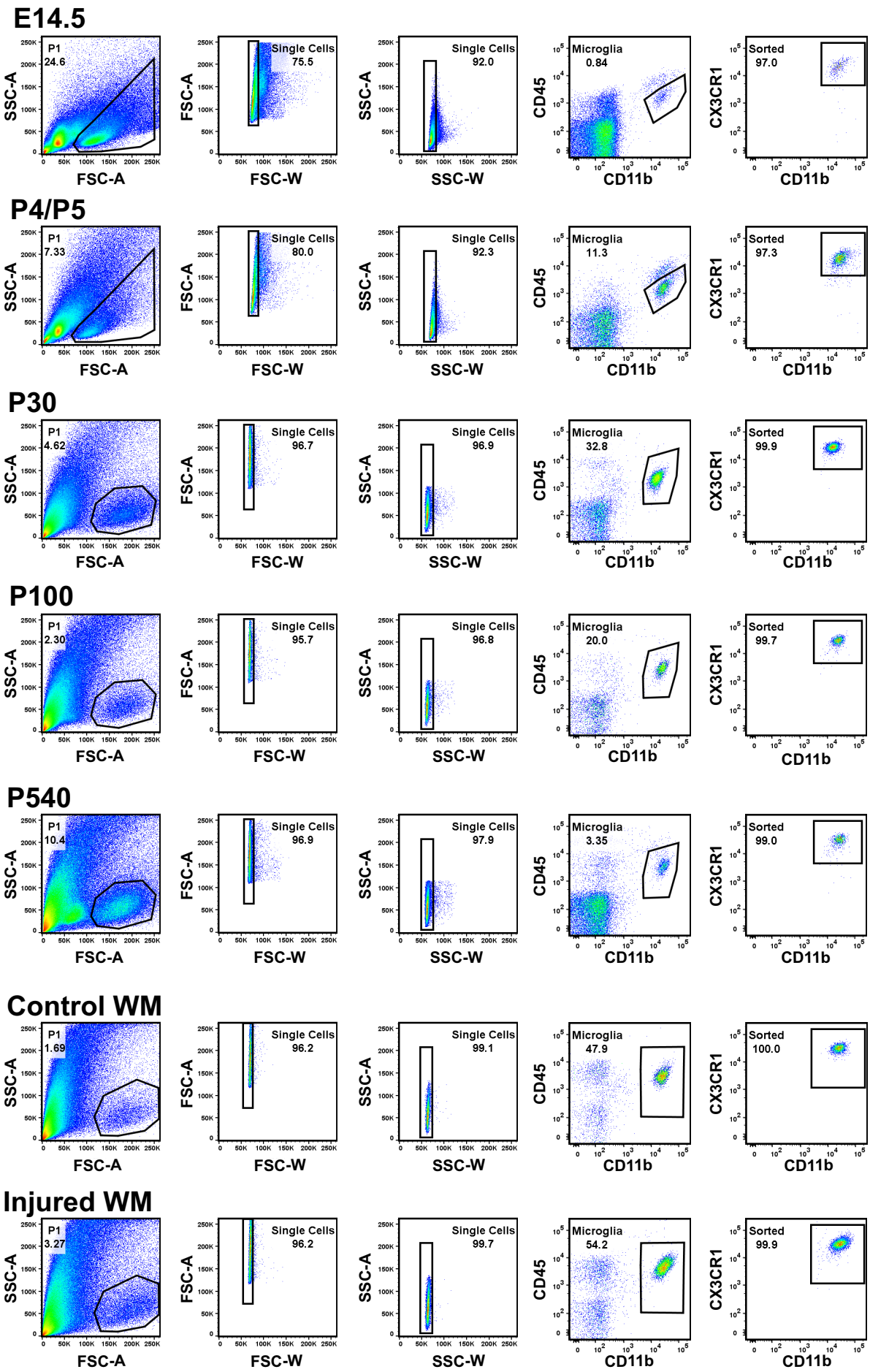

Figure S2. Cell sequencing metrics and ICA removal of contaminating cells and batch-related Ics, related to STAR methods.

(a) Plots of mean reads per cell, median UMIs per cell, and median genes per cell for all sequenced samples. N = 41 mice total, **P<0.01, one-way ANOVA, Tukey's post-hoc analysis.

(b) tSNE plots of all sequenced cells after first round of clustering and before removal of contaminating cells. tSNEs are colored for gene expression (log-transformed UMI counts per 10,000 transcripts) for common neuron/neuroblast markers including *Tubb3, Meg3,* and *Dcx.*

(c) tSNE plots of all sequenced cells after first round of clustering and before removal of contaminating cells colored for common astrocyte marker *Gfap,* OPC/oligodendrocyte marker *Olig1*, and endothelial cell marker *Vtn*.

(d) tSNE plots of all sequenced cells after first round of clustering and before removal of contaminating cells colored for the cell loading values for three major batch-related independent components (ICs). Genes enriched in each IC are listed above each plot.

Supplemental Figure 3

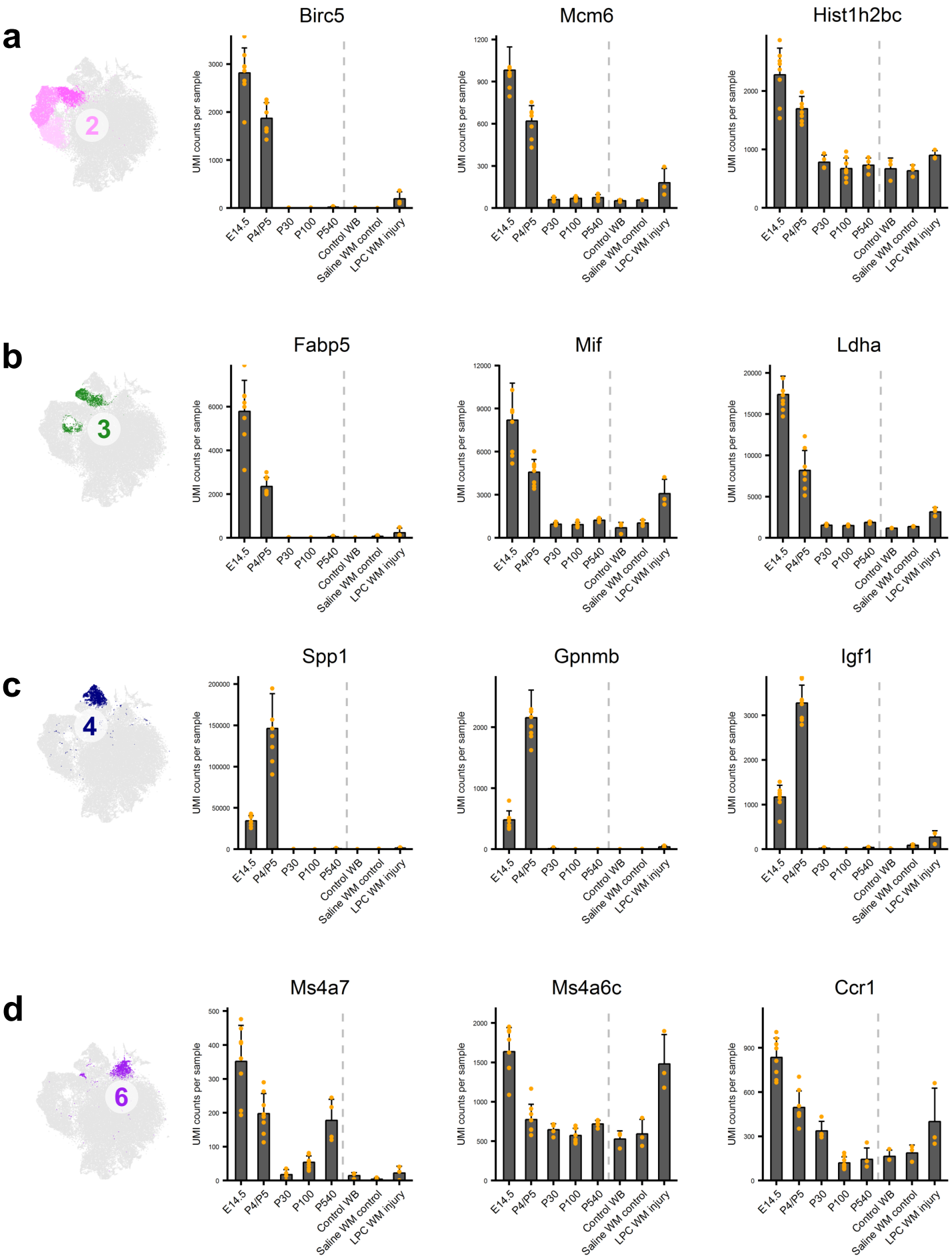

Figure S3. FACS gating strategy for microglia enrichment before single-cell sequencing, related to STAR methods.

Representative FACS plots for 300,000 total events are displayed for animals at each age. Plots are shown in order (left to right) to show the gating strategy used to distinguish cells from debris, to isolate single cells (2), and then to identify microglia by $Cd45^{low}Cd11b^{high}$ and $Cx3cr1^{high}Cd11b^{high}$ expression.

Supplemental Figure 4

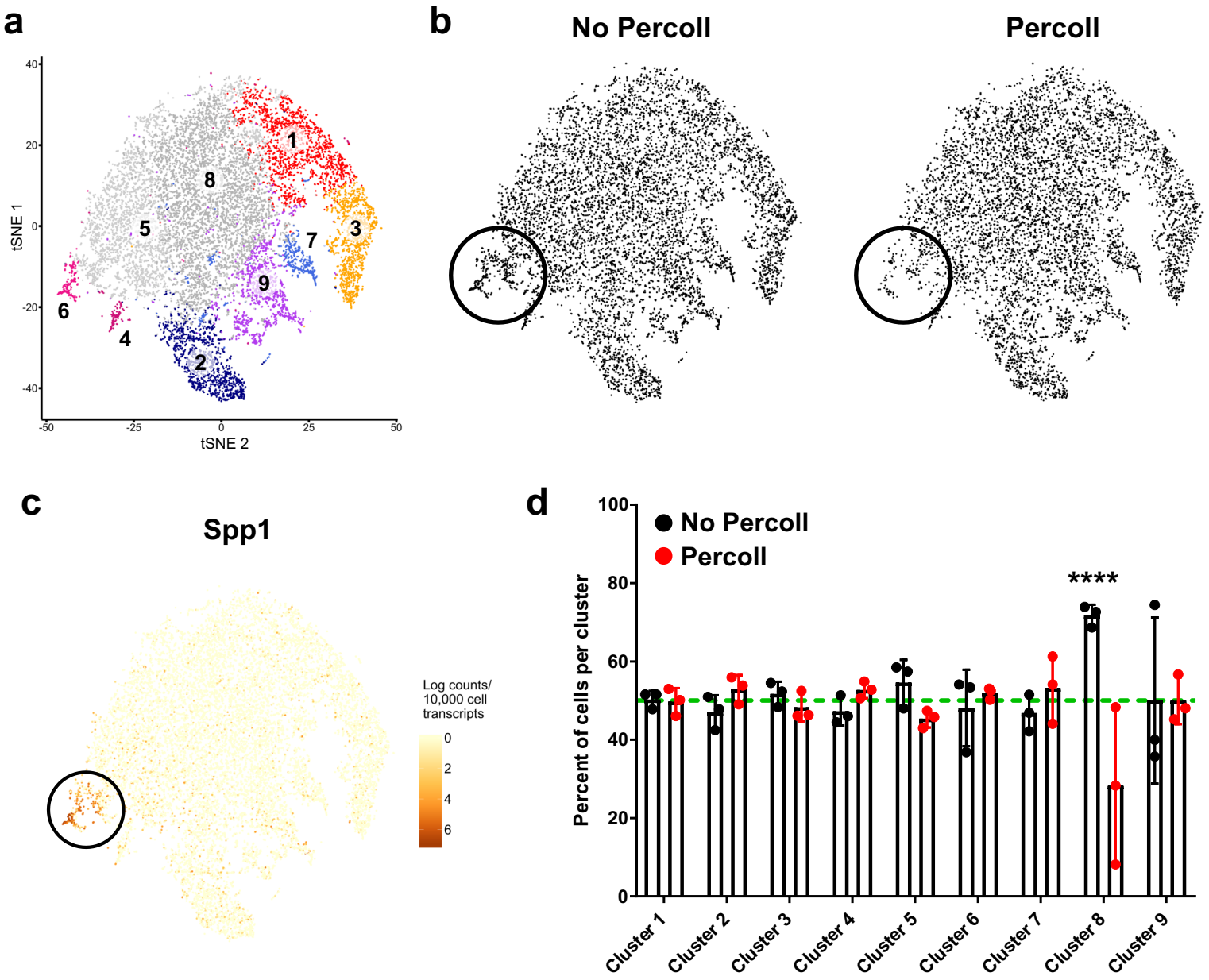

Figure S4. Metacell analysis of cluster marker gene expression changes over time and following injury, related to Figs 2-4.

(a-d) Normalized total gene expression per sample for cluster-specific markers plotted for each timepoint and injury condition. Individual points represent separate animals (N=3-8). Grey dotted line separates normal development from IRM samples.

Supplemental Figure 5

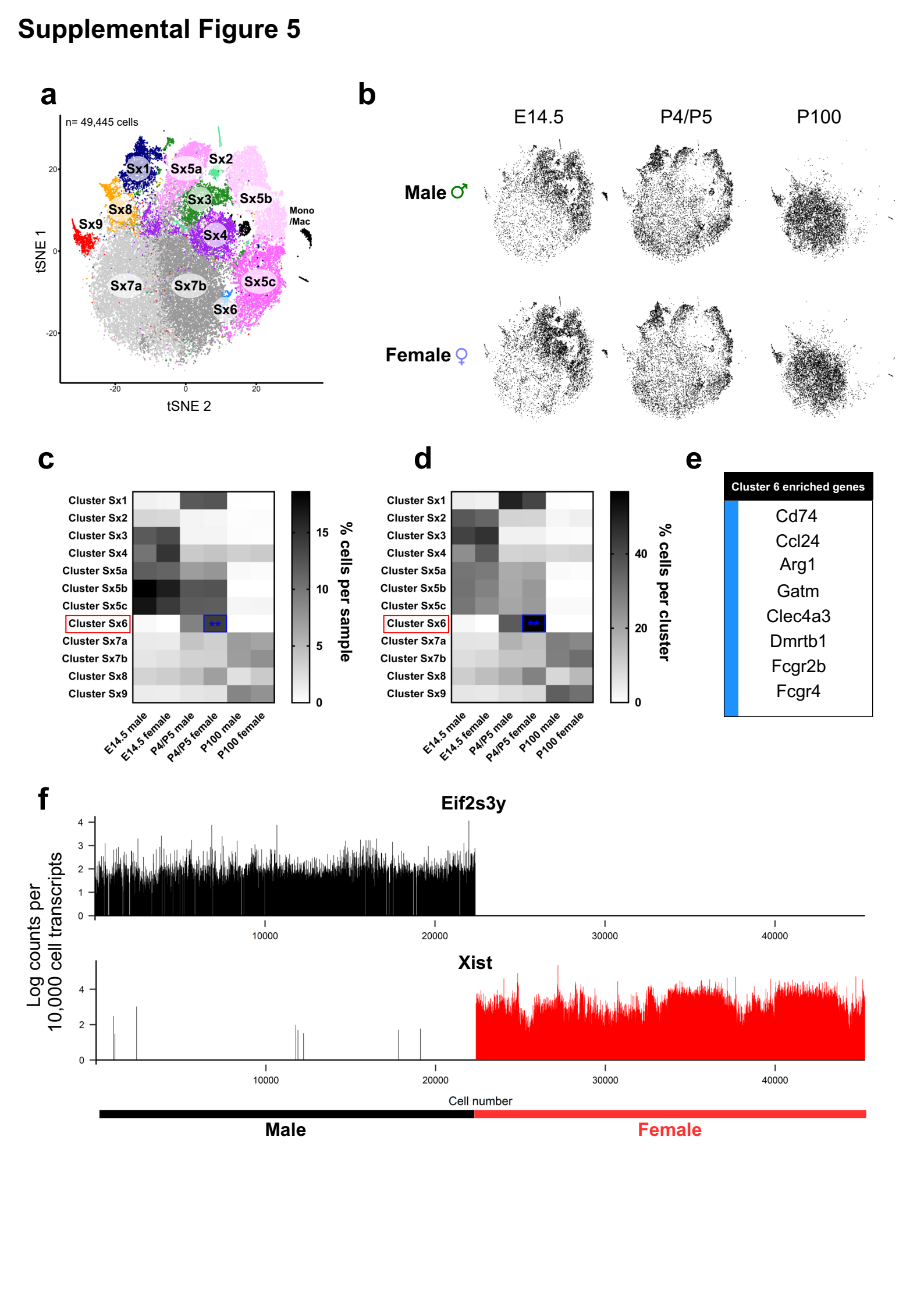

Figure S5. Reactome and Kegg pathway analysis of Cluster 2,3,4 and 6 microglia. Related to Figs 1-4.
(a-f) Reactome pathway analysis of genes enriched 1.5 fold or higher in indicated cluster. The top 15 pathway matches are displayed. Red line denotes an FDR-corrected (Benjamini Hochberg) significance threshold of 1.3 (-log(10)) or 0.05 [untransformed]). Blue bars are from Kegg, black bars are from Reactome.

Supplemental Figure 6

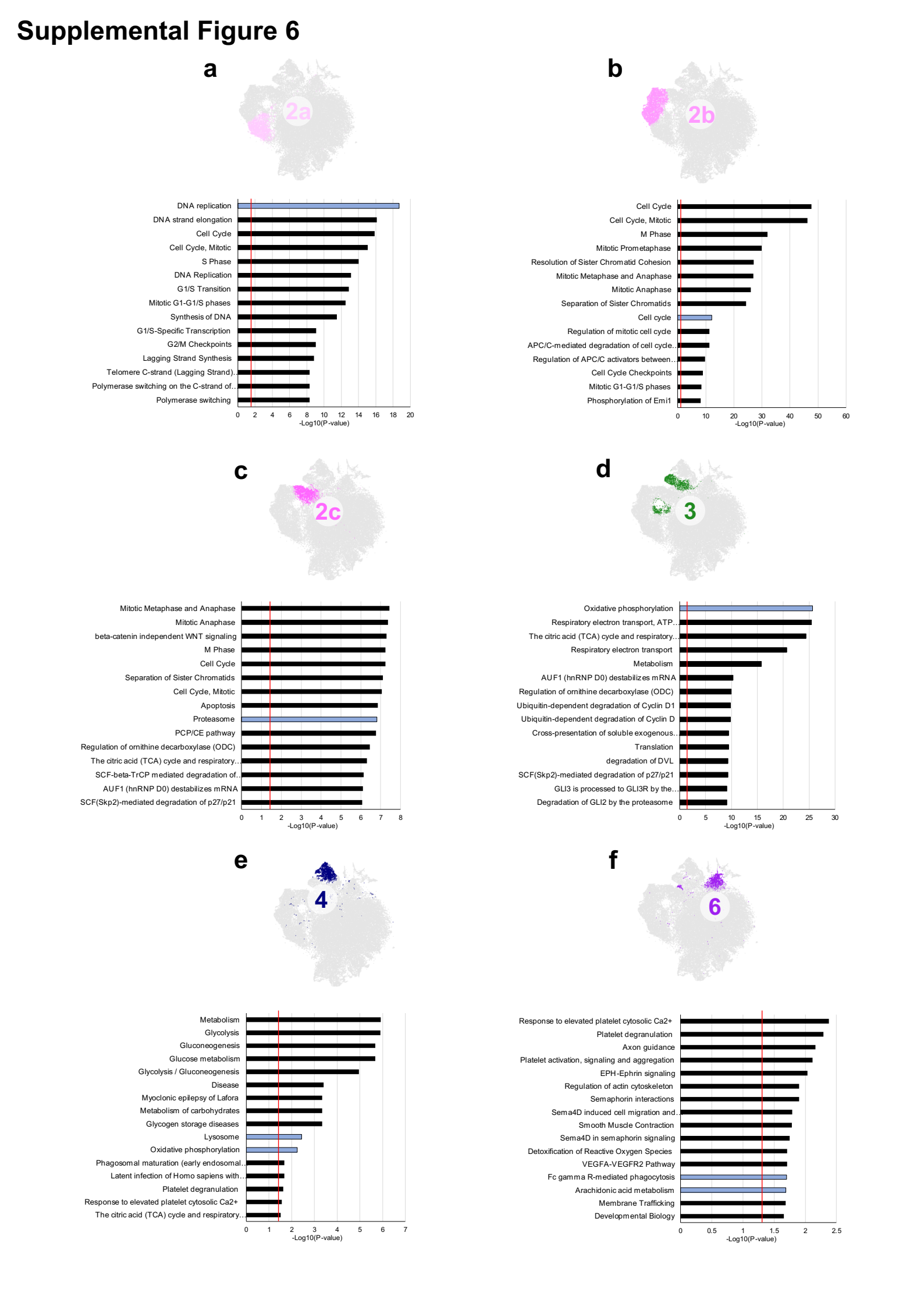

Figure S6. Animal sex has no impact on microglial diversity, related to Fig. 1.
(a) tSNE plot of 49,445 microglia from E14.5 male, E14.5 female, P4/P5 male, P4/P5 female, P100 male, and P100 female mice (N=4 per age and sex) shows nine microglia clusters.
(b) tSNE plots of cells from each age and sex.
(c-d) Heatmap of the percent of cells per sample assigned to each cluster (c) or normalized percent of cells from each sample assigned to each cluster (d). Blue squares = increase in cells for a given age/sex ($P<0.0001$). Two-way ANOVA with Tukey's post-hoc analysis.
(e) List of genes enriched in Cluster 6, which was enriched in female samples at P4/P5.
(f) Plot of the number of log-transformed counts per 10,000 cell transcripts for the Y chromosome gene *Eif2s3y* and X chromosome inactivation gene *Xist* in all 49,445 microglia isolated from male and female samples

Supplemental Figure 7

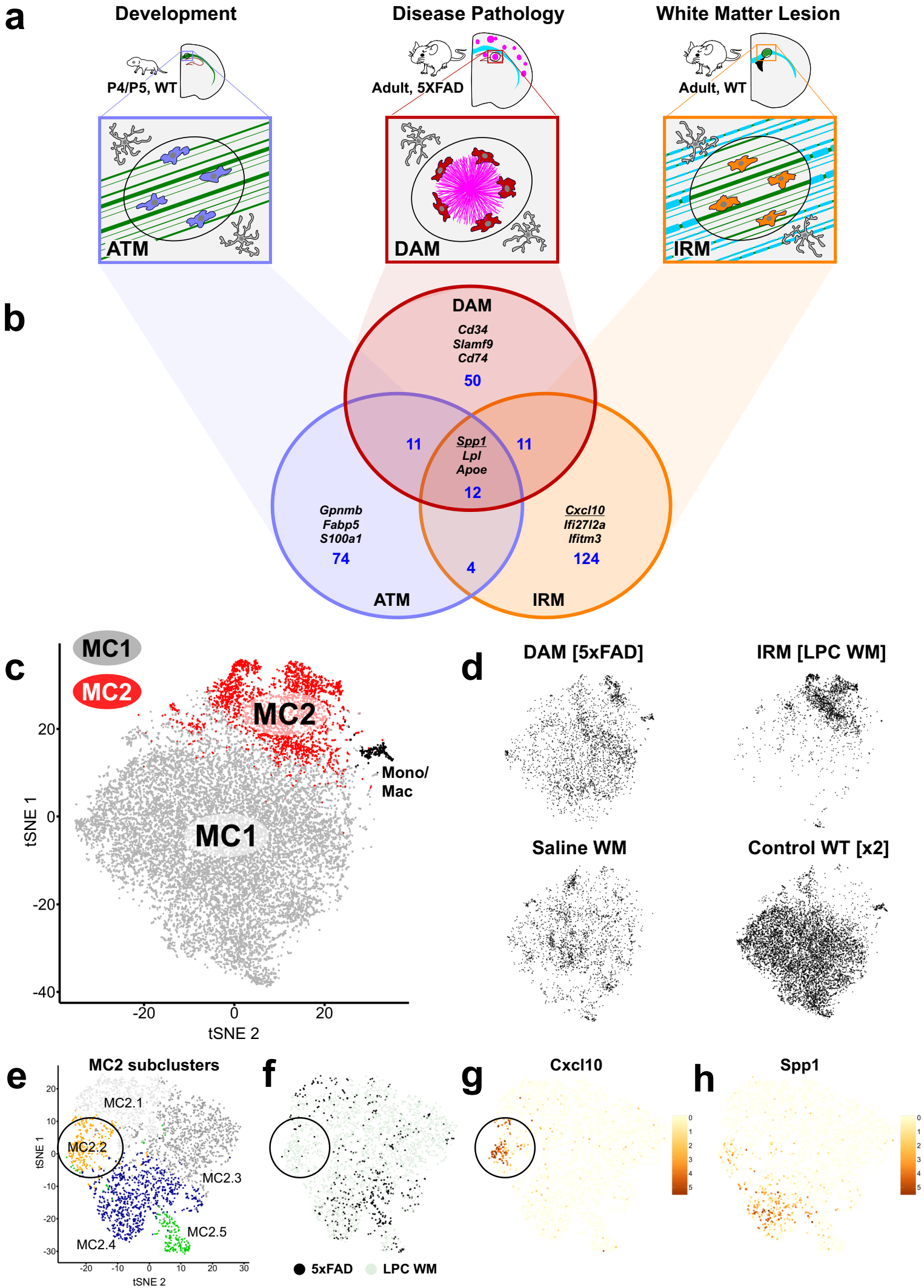

Figure S7. Comparison of microglia activation signatures in development, disease and injury. Related to Fig 6.

(a) Single cell microglia transcripomes from P5 mouse developing axon tract-associated microglia (ATM), adult mouse disease associated microglia (DAM) from Alzheimer's mouse model (Keren-Shaul et. al 2017), and adult injury responsive mouse microglia (IRM) from LPC injected demyelinated white matter were compared.

(b) Genes with a P-value < 1E-10 and fold change > 1.5 versus other microglia (ATM) or control samples (DAM and IRM) were selected from each dataset. Shared and unique genes are present in a Venn diagram with selected genes labeled

(c) Canonical correlation analysis (CCA) was used normalize batch and platform differences and to cluster DAM and IRM. tSNE plot of 19,792 microglia reveals two microglia clusters (microglia comparison 1 and 2 (MC1, MC2) and one Mono/Mac cluster. N=3-4 mice per condition.

(d) tSNE plots of cells from each condition. Control WB and control WT (Keren-Shaul et. al 2017) were pooled (Control WT x2).

(e) Cells from Cluster MC2 were subclustered to identify different subpopulations of activated microglia. tSNE plot shows five subclusters of Cluster MC2 microglia (MC2.1-MC2.5).

(f) tSNE plot of subclustered cells from 5xFAD (black) and LPC WM (grey) mice.

(g) tSNE plot of subclustered cells colored for *Cxcl10* gene expression (log-transformed transcripts per million (TPM)).

(h) tSNE plot of subclustered cells colored for *Spp1* gene expression (log-transformed transcripts per million (TPM)).

Supplemental Table 1. Upregulated and downregulated genes, including transcription factors, for each cluster from Figure 1, Figure 5, and Figure 6. Fold changes, Pvalue, FDR corrected adjusted pvalue (Padj FDR), and the percent of cells in the cluster of interest (pct.1) versus all other cells (pct.2) are shown.

Supplemental Table 2. Gene overlap comparison between the Disease Associated Microglia (DAM, Keren Shaul et al. 2017), Injury Responsive Microglia (IRM) and P5 Axon Tract Associated Microglia (ATM). Related to Figure 6 and Figure S7. Unique and overlapping genes are noted.

Supplemental Table 3. Patient information from control and Multiple Sclerosis human brain samples. Related to Figure 7.